

Annual Evaluation of Supply–Demand with BESS Charging/Discharging Schedule and UC Updating Based on Intraday Forecasted PV Power Outputs

Taisuke Masuta, Daiki Kobayashi
Meijo University
Nagoya, Japan
masuta@meijo-u.ac.jp
130442063@cgalumni.meijo-u.ac.jp

Nguyen Hoang Viet
Hanoi University of Science and
Technology
Hanoi, Vietnam
viet.nguyenhoang1@hust.edu.vn

Hideaki Ohtake
National Institute of Advanced
Industrial Science and Technology
Tsukuba, Japan
hideaki-ootake@aist.go.jp

Abstract—In recent years, photovoltaic (PV) systems have been installed in Japan at an accelerated rate. The application of PV generation forecasts and the utilization of energy storage devices in power system operation are essential to reduce supply–demand imbalances and enable the use of more PV energy without curtailment. In this paper, assuming extremely high PV generation after 2030, we focus on the coordinated operation of a battery energy storage system (BESS) and conventional power plants. We propose a method of determining and updating the BESS charging/discharging schedule and generator unit commitment based on the day-ahead and intraday PV generation forecasts. We present an evaluation of this method based on the results of numerical simulations conducted for one year on a bulk power system model to demonstrate the effectiveness with which it reduces energy shortfall and PV power curtailment.

Index Terms—Battery energy storage system (BESS); photovoltaic (PV) generation; PV generation forecast; power system; unit commitment (UC)

I. INTRODUCTION

In Japan, the installed capacity of renewable energy systems such as wind and photovoltaic (PV) power systems has been increasing rapidly due to the feed-in tariff policy, which started in 2012. In particular, PV systems have been installed at an accelerating rate. The accumulated installed capacity reached 20 GW at the end of 2015, and the governmental target is set to 64 GW in 2030 [1]. However, taking their low capacity factors into account, 64 GW of PV systems can supply only approximately 6% of the total electricity needed in Japan. Our research group has developed power system control and operation methods based on PV generation forecasts assuming future power systems with extremely high PV system integration, targeting a total installed PV capacity in Japan of 100–300 GW [2]. Although the application of renewable power generation forecasting to power systems in Japan has been investigated in numerous studies [3], [4], extremely high integration cases in which the PV power output could be greater than the maximum load

demand of the entire power system were not considered in most of them. In such power systems, numerous problems must be solved such as supply–demand operation, transmission control, distribution control, etc. In this study, we focused on supply–demand operation for power systems with extremely high PV generation.

PV systems are uncertain power sources whose power outputs are not controllable and that generate power only during the daytime. It is important for power systems to be both reliable, thereby decreasing the power imbalances caused by uncertain outputs, and energy efficient, thereby utilizing as much PV energy generated during the daytime as possible. Accurate PV power output forecasting is necessary for reliability, and energy storage devices are essential for energy efficiency. A method for updating the unit commitments (UCs) of thermal generators based on intraday PV generation forecasts was proposed in [3], and such short-interval UCs have been implemented practically [5]. Although the proposed method was evaluated by performing a one-day simulation [3], longer evaluation periods such as one year are necessary because solar irradiation and load demands vary significantly from day to day, and from season to season. The operation methods of generators with energy storage systems including UCs have been conventionally investigated [6], [7]; however, load leveling was targeted in those studies. Although a battery scheduling method considering forecasts was presented in [8], it was intended for consumers or prosumers to reduce buying cost and increase selling interest. Thus, the coordinated operation of generators and storage systems for utilizing renewable energy adequately to reduce supply–demand imbalances in large power systems has rarely been investigated

We previously developed supply–demand operation methods with battery energy storage systems (BESSs) based on PV generation forecasts [9]–[11]. In those studies, we proposed and evaluated an operation method that decreases supply–demand imbalances by updating the UCs of thermal power generators based on both day-ahead and intraday PV

This work was partly supported by JST CREST Grant Number JPMJCR15K1 (5, Sanbancho, Chiyoda-ku, Tokyo, 102-0075, Japan) and Meijo Asian Research Center (1-501 Shiogamaguchi, Tempaku-ku, Nagoya, 468-8502, Japan).

generation forecasts [9], a BESS operation method based on PV generation forecasts for efficient use of generated PV energy [10], and a coordinated operation method for thermal generators and a BESS assuming the PV installation target in 2030 (a total of 64 GW in Japan) [11]. In this paper, expanding upon the method proposed in [11], we propose a supply–demand operation method with updating of the BESS charging/discharging schedule and UC of the thermal power generators based on both day-ahead and intraday PV power output forecasts released every 6 h, assuming extremely high PV generation after 2030 (a total of 300 GW in Japan). Although evaluations of the proposed methods for two months during the light-load season were presented in [9]–[11], in this study, we evaluated the proposed method based on the reliability and energy efficiency of the supply–demand operation for one year by conducting numerical simulations on a model of the power system in the Kanto area of Japan, which includes Tokyo city and is the largest power system in Japan. In addition, we evaluated the impact of the installed PV capacity on the proposed operation method, considering the installed PV capacity as a parameter.

II. DETERMINATION AND UPDATING OF BESS SCHEDULE AND UC

In this paper, we assume a large power system that consists of numerous conventional power plants such as thermal, nuclear, and hydropower plants; plenty of PV generation; and a large BESS. We focus on the daily supply–demand operation for numerous thermal generators and a BESS. (The power outputs of nuclear and hydropower plants are assumed to be constant.) We also assume that the BESS is used not for reserve capacity to avoid outages or to compensate for short-term power fluctuations, such as in load frequency control (LFC), but rather for efficient use of PV energy when it is expected to be surplus; that the inverter and battery capacities of the BESS are sufficient; and that the initial and final states of charge (SOCs) of the BESS are identical on each day. Fig. 1 shows a time chart of the determination and updating of the charging/discharging schedule of the BESS and UC of the generators.

Firstly, after checking the constraints of the upper limits of the PV power output and BESS discharging power in each time period based on the forecasts released at 12 local time (LT) on the previous day, the charging/discharging schedule

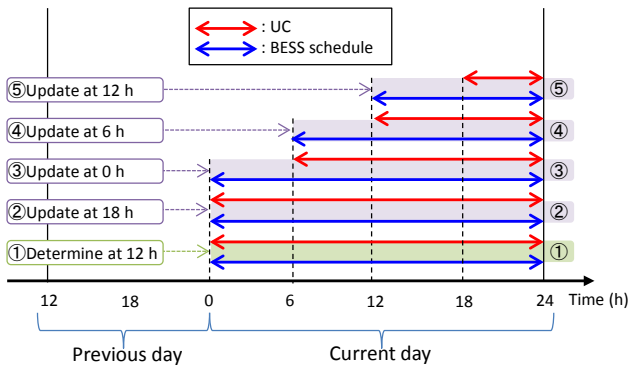


Figure 1. Time chart of BESS schedule and UC determination/updating.

and UC are determined. Then, after checking the constraints of the upper limits again based on the latest forecasts released every 6 h, the charging/discharging schedule and UC are repeatedly updated. (The UC is determined or updated just after the BESS schedule is determined or updated.) We assume that the load demand can be forecasted with high accuracy at 12 LT on the previous day.

A. Constraints of Upper Limit of PV Power Output

The number of thermal generators at time j , N_j^G , should satisfy the following three equations to avoid short-term large power flow fluctuations and power shortfalls or surplus with adequate regulating capacity [11], [12]. Here, the thermal generators start in the order $i = 1, 2, \dots, N_j^G$.

$$\sum_{i=1}^{N_j^G} C_i^{LFC} + C^H \geq R^D \cdot P_j^D + R^R \cdot P_j^{PV}, \quad (1)$$

$$P_j^D - P_j^{PV} - P^{NU} - P^H \geq \sum_{i=1}^{N_j^G} (P_i^{MIN} + C_i^{LFC}), \quad (2)$$

$$P_j^D - P_j^{PV} - P^{NU} - P^H \leq \sum_{i=1}^{N_j^G} (P_i^{MAX} - C_i^{LFC}), \quad (3)$$

where C_i^{LFC} is the LFC regulating capacity of generator i ; C^H is the total LFC regulating capacity of hydropower generators; P_j^D is the total load demand at time j ; P_j^{PV} is the total PV power output at time j ; R^D and R^R are the ratios of the required LFC regulating capacities to the load demand and the PV power output, respectively; P^{NU} and P^H are the total power outputs of nuclear and hydropower plants, respectively; and P_i^{MIN} and P_i^{MAX} are the minimum and maximum outputs of thermal generator i , respectively.

Eq. (1) is the constraint for securing LFC regulating capacity, while (2) and (3) are the constraints for maintaining supply–demand balance. The PV output is maximized with the smallest N_j^G that satisfies (1)–(3), which is the upper limit of the PV power output in the time period. Eqs. (1) and (2) can be transformed into (4) and (5), which represent the facts that the PV power output is restricted by the LFC regulating capacity constraint or the supply–demand balance constraint, respectively. The smaller of the maximum PV power outputs in (4) and (5) is defined as the upper limit of the PV power output, $P_j^{PV_MAX}$. In this study, before determining or updating the BESS schedule and the UC, the hourly upper limits of the total PV power output in each time period after the released time of the forecasts were calculated.

$$P_j^{PV} \leq \frac{1}{R^R} \cdot \left(\sum_{i=1}^{N_j^G} C_i^{LFC} + C^H - R^D \cdot P_j^D \right) \quad (4)$$

$$P_j^{PV} \leq P_j^D - P^{NU} - P^H - \sum_{i=1}^{N_j^G} (P_i^{MIN} + C_i^{LFC}) \quad (5)$$

B. Setting of Upper Limit of BESS Discharging Power

We assume that the BESS charges while the PV power output is forecasted to be surplus and discharges during the other periods. Thus, the supply–demand balance can be represented as (6) during BESS charging or PV curtailment and (7) during the other periods;

$$P_j^D = \sum_{i=1}^{N_G} P_{i,j}^G + P^{NU} + P^H + (P_j^{PV} - P_j^{Charge} - P_{i,j}^{PV-C}), \quad (6)$$

$$P_j^D - P_j^{Discharge} = \sum_{i=1}^{N_G} P_{i,j}^G + P^{NU} + P^H + P_j^{PV}, \quad (7)$$

where $P_{i,j}^G$, P_j^{PV-C} , P_j^{Charge} , and $P_j^{Discharge}$ are the power output of thermal generator i , curtailed PV power, and charging and discharging powers of the BESS at time j , respectively. As shown by transforming (7) into (8), the upper limit of the discharging power $P_j^{Discharge_MAX}$ exists during each time period. Thus, the integral of the upper limit of the discharging power for a day is that of the discharging energy in a day, considering the constraint that the initial and final SOCs of the day are identical.

$$\begin{aligned} P_j^{Discharge} &= P_j^D - \left(\sum_{i=1}^{N_G} P_{i,j}^G + P^{NU} + P^H + P_j^{PV} \right) \\ &\leq P_j^D - \left(\sum_{i=1}^{N_G} (P_i^{MIN} + C_i^{LFC}) + P^{NU} + P^H + P_j^{PV} \right) = P_j^{Discharge_MAX} \end{aligned} \quad (8)$$

C. Charging Schedule

Based on the latest forecasts while determining or updating the schedule, the BESS charges when the PV power output is forecasted to be larger than the upper limit mentioned in Section II-A. Firstly, the charging schedule is determined or updated assuming that the total power over the upper limit can be charged according to

$$P_j^{Charge} = \max(0, P_j^{PV0} - P_j^{PV_MAX}), \quad (9)$$

where P_j^{PV0} is the potentially available PV power output before charging or curtailment at time j . Secondly, the total charging energy in a day is compared with the integral of the upper limit of the discharging power. If it is larger, the charging power is modified and the curtailed power is set as

$$\begin{cases} \text{if } \eta \cdot \sum_{j=1}^T P_j^{Charge} \cdot \Delta T \geq \sum_{j=1}^T P_j^{Discharge_MAX} \cdot \Delta T \\ P_j^{Charge} = (P_j^{PV0} - P_j^{PV_MAX}) \cdot \frac{\sum_{j=1}^T P_j^{Discharge_MAX} \cdot \Delta T}{\eta \cdot \sum_{j=1}^T (P_j^{PV0} - P_j^{PV_MAX}) \cdot \Delta T} \\ P_j^{PV-C} = P_j^{PV0} - P_j^{PV_MAX} - P_j^{Charge} \quad (j = t, t+1, \dots, T) \end{cases}, \quad (10)$$

where η is the charging efficiency of the BESS; t is the time at which the forecast is released; ΔT and T are the time unit and scheduling period, respectively ($\Delta T = 1$ h and $T = 24$ h in this study).

D. Discharging Schedule

After determining or updating the charging schedule, the discharging schedule is determined or updated by employing quadratic programming, where the objective is to minimize [11]

$$f^{Discharge} = \sum_{j=t}^T (P_j^D - P_j^{PV} - P_j^{Discharge})^2 \cdot \Delta T. \quad (11)$$

Here, $f^{Discharge}$ represents the squared sum of the power supplied by the power plants other than those that generate PV power. Minimizing $f^{Discharge}$ is intended to reduce the operational cost of the thermal generators by leveling the gross daily load curve. The constraints include the prohibition of simultaneous charging and discharging, the balance between the charging and discharging energies in a day, and the initial and final conditions of the stored energy.

The BESS does not discharge when it charges, since

$$P_j^{Discharge} = 0 \quad \text{if } P_j^{Charge} > 0. \quad (12)$$

The constraint of the balance between the charging and discharging energies is given by

$$\eta \cdot \sum_{j=1}^T P_j^{Charge} \cdot \Delta T = \sum_{j=1}^T P_j^{Discharge} \cdot \Delta T. \quad (13)$$

The stored energy at time j , E_j^{BESS} can be expressed as

$$E_j^{BESS} = E_0^{BESS} + \eta \cdot \sum_{j'=1}^j P_{j'}^{Charge} \cdot \Delta T - \sum_{j'=1}^j P_{j'}^{Discharge} \cdot \Delta T. \quad (14)$$

The constraint of the initial and final conditions of the stored energy is given by

$$E_0^{BESS} = E_T^{BESS}. \quad (15)$$

Although it is a strict constraint, we have considered it to evaluate the proposed method in terms of the daily scheduling and operation.

E. Decision Variables in Schedule Updating

The decision variables involved in determining or updating the charging/discharging schedule discussed in Sections II-C and II-D are P_j^{Charge} and $P_j^{Discharge}$. The values from time $j = 1$ to T are obtained in the first determination and those from time $j = t$ to T are obtained in the subsequent updates. In the updates, P_j^{Charge} and $P_j^{Discharge}$ before the forecast release time are not decision variables, but rather fixed values obtained during the previous scheduling.

F. UC of Thermal Generators

The UC of the thermal generators is determined or updated by employing dynamic programming, where the objective is to minimize [11], [13]

$$f^G = \sum_{i=1}^N \sum_{j=1 \text{ or } t+6}^T \{u_{i,j} \cdot FC_i(P_{i,j}^G) \cdot \Delta T + u_{i,j} \cdot (1 - u_{i,j-1}) \cdot SC_i\}, \quad (16)$$

where FC_i and SC_i are the fuel cost function and startup cost of generator i , respectively; N is the total number of thermal generators; and $u_{i,j}$ is the operation state of thermal generator i at time j ($u_{i,j} = 1$: operating, 0 : stopped). The scheduling period is from $j = 1$ to T in the determination and from $j = t + 6$ to T in the subsequent updates. The margin to start up the thermal generators after updating the schedules is 6 h. The constraints include the supply–demand balance, upper/lower limits of the thermal generators, upward reserve capacity, LFC regulating capacity, and priority dispatch for PV generation. The supply–demand imbalance constraint considers the charging and discharging powers and PV curtailment obtained in the latest BESS schedule.

III. CURRENT DAY OPERATION OF BESS, THERMAL GENERATORS, AND PV SYSTEMS

A. BESS Charging and Discharging

In the current day operation, the BESS charges or discharges by following the latest schedule at the time [11]. It is not used for emergency control to reduce sudden supply–demand imbalances.

B. Optimal Load Dispatch for Thermal Generators

In the current day operation, the thermal generators start or stop following the latest UC at the time [11]. The load dispatch for each generator is obtained by employing quadratic programming, where the objective is to minimize the total fuel cost of all of the operating generators [11], [13]. The constraints include the supply–demand balance considering the actual PV power output and charging/discharging power of the BESS; upper and lower limits of the generators; LFC regulating capacity; and priority dispatch for PV generation.

C. Supply-Demand Imbalances

If output greater than the total maximum output is requested of the operating thermal generators when the supply–demand balance differs from the schedule due to forecasting error, power shortfall will occur. The power shortfall at time j , $P_j^{\text{Shortfall}}$, is given by

$$P_j^{\text{Shortfall}} = P_j^D + P_j^{\text{Charge}} - P_j^{\text{Discharge}} - \left\{ P_j^{\text{PV}} + P^{\text{NU}} + P^{\text{H}} + \sum_{i=1}^{N^G} (P_i^{\text{MAX}} - C_i^{\text{LFC}}) \right\}. \quad (17)$$

We assume that each PV system can curtail its output by the amount requested by the system operator in real time. If the PV power output is greater than the scheduled charging

power during the time that the BESS charging is scheduled, the PV power output is curtailed. In this situation, the PV power curtailment at time j , $P_j^{\text{PV}-C}$, is given by

$$P_j^{\text{PV}-C} = P_j^{\text{PV}} - P_j^{\text{Charge}}. \quad (18)$$

If the PV power output is greater and (1) or (2) is not satisfied considering the discharging power during the time that BESS charging is not scheduled, the PV power output is also curtailed. In this case, $P_j^{\text{PV}-C}$ is given by

$$P_j^{\text{PV}-C} = P_j^{\text{PV}} - P_j^{\text{PV}-\text{MAX}}. \quad (19)$$

IV. NUMERICAL SIMULATIONS

A. Simulation Conditions

Numerical simulations were conducted on a power system model of the Kanto area in Japan. (The maximum load demand is approximately 60 GW, which is one third of the total in Japan.) We assumed the future power system after 2030, in which the installed PV generation capacity will continue to increase. The available capacities of the power plants are shown in Table I. The UC targets were 168 thermal generators with the specifications described in [13]. The thermal generators started up in order of ascending fuel cost at the rated output, and 5% of the rated output of each operating generator was available for the LFC regulating capacity. The total output of the hydropower plants was assumed to be constant at 95% of the available capacity, and the remaining 5% was available for the LFC regulating capacity. The total output of the nuclear power plants was assumed to be constant at 100% of the available capacity during peak-load season (from July 15 to Sept. 14) and 66.7% during the other seasons. The ratios of the required LFC regulating capacities to the load demand and PV power output were both 2%. The ratio of the upward reserve capacity was 3% of the load demand. The installed capacity of the PV generation was considered as a parameter which changes from 0 GW to 100 GW, that corresponds to approximately from 0 GW to 300 GW of all Japan. The BESS capacity was assumed to be sufficient. The charging efficiency was 80%.

The simulation period was one year, and the time unit was 1 h. We used the hourly actual load demand data of the Kanto area in 2010 [14], the hourly actual solar irradiation data averaged over the six sites in the Kanto area in 2010 [15]. The PV power output was obtained by multiplying the normalized solar irradiation times the installed PV capacity and system coefficient (0.8 in this study) [9]–[11], [13]. We employed the hourly forecasted solar irradiation data from the

TABLE I. AVAILABLE CAPACITIES OF POWER PLANTS

	Available capacity [MW]	
	Jul. 15 -Sept. 14	Other
Nuclear	9,000	6,000
Hydro	1,200	
Thermal	60,850 (168 machines)	

abovementioned six sites calculated by AIST using the source code of a mesoscale model developed by the Japan Meteorological Agency [16], [17]. The hourly forecasts of the current day were released at 12 and 18 LT on the previous day and 0, 6, and 12 LT on the current day. The later the forecast release, the smaller the forecasting error [9]-[11], [16].

We implemented three cases in the simulations. In Case 1, the charging/discharging schedule of the BESS and the UC of the generators were determined based on the forecasts released at 12 LT on the previous day and were not updated (Base case). In Case 2, the charging/discharging schedule and UC were determined and updated based on the forecasts released at 12 and 18 LT on the previous day and 0, 6, and 12 LT on the current day (Proposed case). In Case 3, assuming the forecasts to be completely accurate, the charging/discharging schedule and the UC were determined based on the perfect forecasts released at 12 LT on the previous day (Reference case).

B. Simulation Results

Although the objective function is the minimization of the operational cost as given in (16), the discussion of the cost for each case has little value because the cost decreases due to power shortfall. Therefore, we mainly focus on the simulation results of supply-demand imbalances in this section.

Figs. 2–4 show the annual total energy shortfall, PV energy curtailment, and PV energy generation loss for each case and various PV installed capacities. The PV energy generation loss was obtained as the sum of the PV energy curtailment and the charge/discharge loss of the BESS [11]. It is important to evaluate the loss when considering BESS installation. In Fig. 2, the shortfall in Case 2 is smaller than that in Case 1 when the installed capacity is less than 60 GW, which demonstrates the effectiveness of the proposed method.

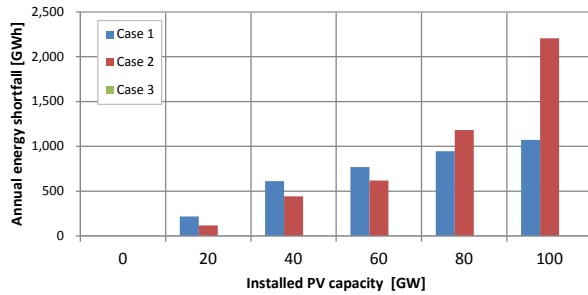


Figure 2. Annual total energy shortfall.

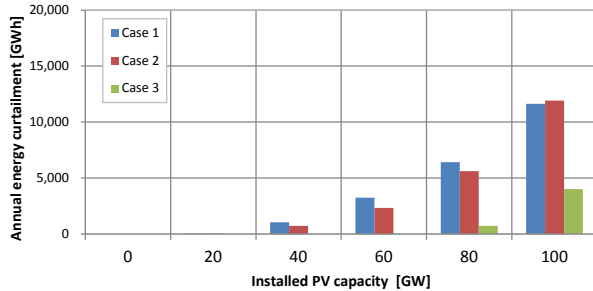


Figure 3. Annual total PV energy curtailment.

Case 1 when the installed PV capacity is extremely large. The reason will be presented in the latter part of this section. In Figs. 3 and 4, the effectiveness of the proposed method is evidenced by the facts that the curtailment and loss in Case 2 tend to be smaller than those in Case 1. However, they are almost the same when the installed PV capacity is 100 GW. In contrast to energy shortfall, PV curtailment can be seen even in Case 3 when the installed PV capacity is greater than 80 GW because the charging power of the BESS is restricted by the constraint of (10).

Figs. 5 and 6 present the monthly total energy shortfall and PV energy curtailment for each case when the installed PV capacity is 40 GW or 100 GW. Although the shortfall in Case 2 tends to be smaller than that in Case 1 in Fig. 5a, Fig. 5b shows a reverse trend particularly around May. In addition, the curtailments from April to June in Case 2 are larger than those in Case 1 in Fig. 6b. It was concluded that if the installed PV capacity is extremely large, the effectiveness of the proposed method is limited during such seasons, when the irradiation is very strong and the entire energy surplus cannot be charged and discharged during one day due to (8)-(10).

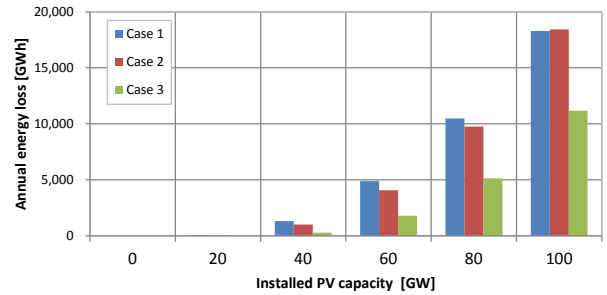
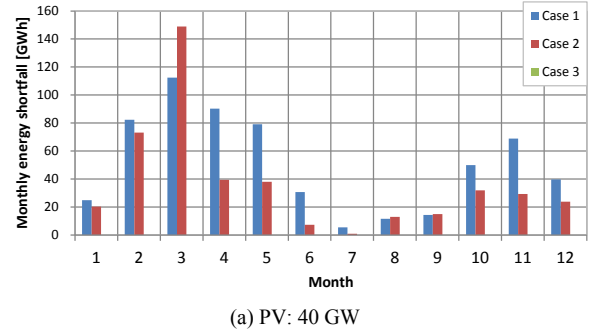
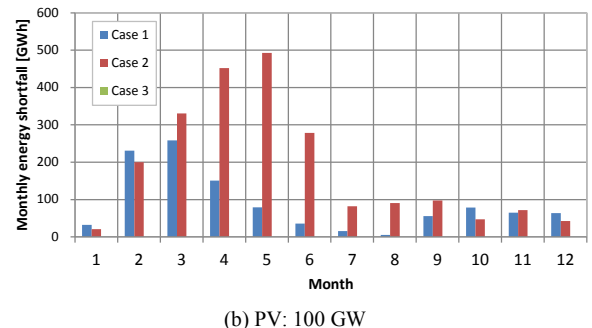


Figure 4. Annual total PV energy generation loss.



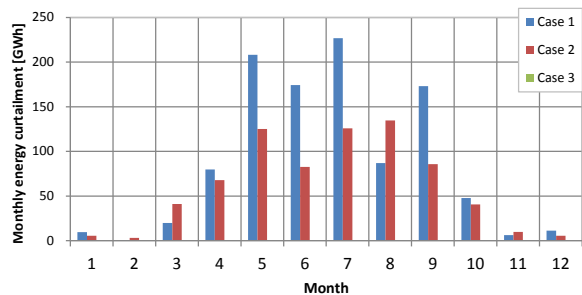
(a) PV: 40 GW



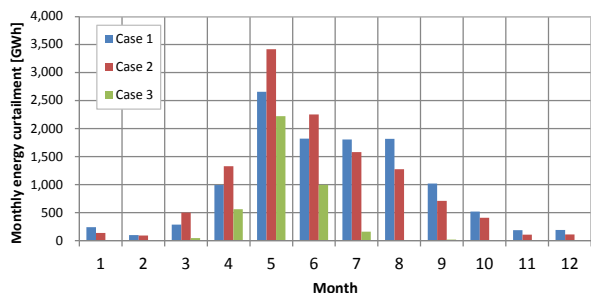
(b) PV: 100 GW

Figure 5. Monthly total energy shortfall

Figs. 7 and 8 show the required inverter and battery capacities of the BESS for each case and various PV installed capacities. The required inverter capacity was obtained as the maximum charging or discharging power in one year. The required battery capacity was calculated as twice the maximum stored energy during a day through one year assuming the initial and final SOCs to be 50%. In Figs. 8 and 9, both the inverter and battery capacities increase with increasing installed PV capacity. In Figs. 7 and 8, the capacity



(a) PV: 40 GW



(b) PV: 100 GW

Figure 6. Monthly total PV energy curtailment.

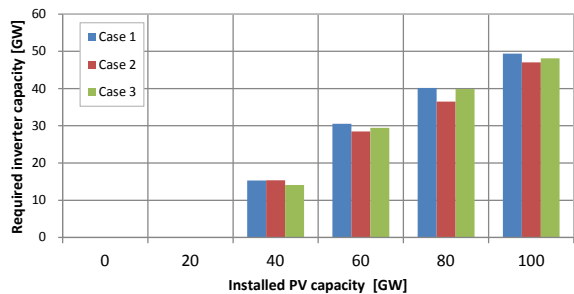


Figure 7. Inverter capacity of BESS.

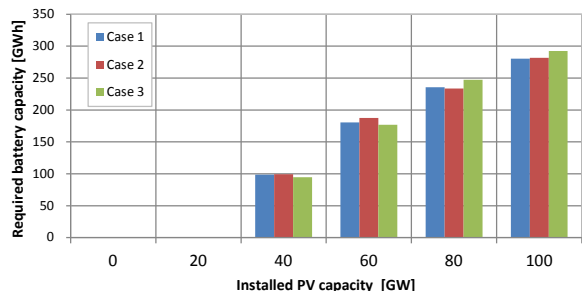
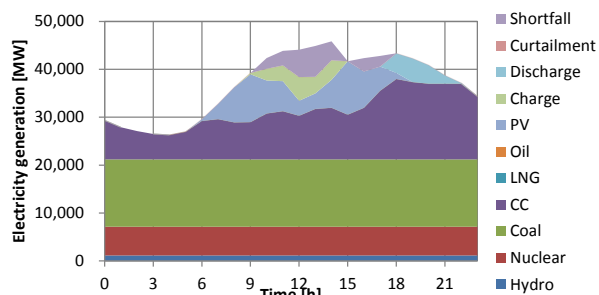


Figure 8. Battery capacity of BESS.

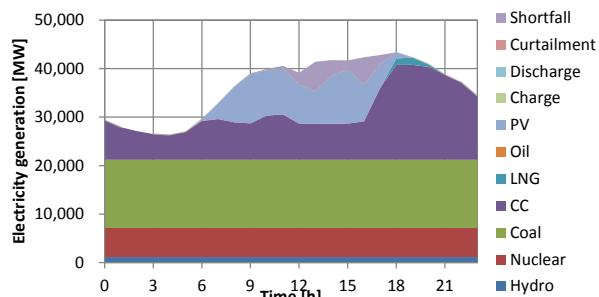
in Case 3 is not always the smallest because the BESS sometimes charges higher energy in Case 3 than in Cases 1 and 2 with the under-forecasted errors.

Fig. 9 presents the daily load curves on April 7, when the installed PV capacity is 100 GW and the proposed method is effective. The generation types, BESS charging/discharging, PV curtailment, and shortfall are color-coded. In Case 1, the BESS operated because the PV power outputs were over-forecasted at 12 LT on the previous day. In Case 2, the BESS schedule was updated not to operate and the charging loss was avoided. In addition, the shortfall decreases from Case 1 to Case 2 to Case 3.

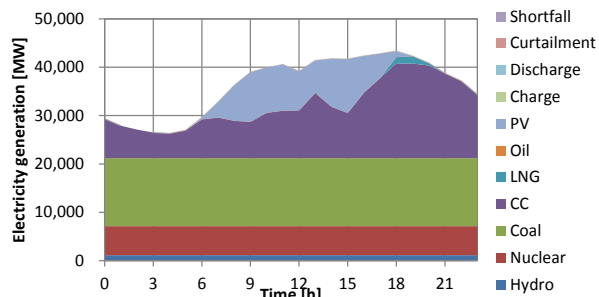
Fig. 10 presents the daily load curves on March 22, when the installed PV capacity is 100 GW and the proposed method is not effective. Curtailment is evident even in Case 3 because a BESS cannot discharge if all of the surpluses are charged, as shown in Fig. 3. The charging energy in Case 1 is almost the same as that in Case 3. The curtailment increases from Case 1 to Case 2 because the PV power outputs were under-forecasted on the current day. A power shortfall occurred from



(a) Case 1



(b) Case 2



(c) Case 3

Figure 9. Daily load curve on April 7 (PV: 100 GW).

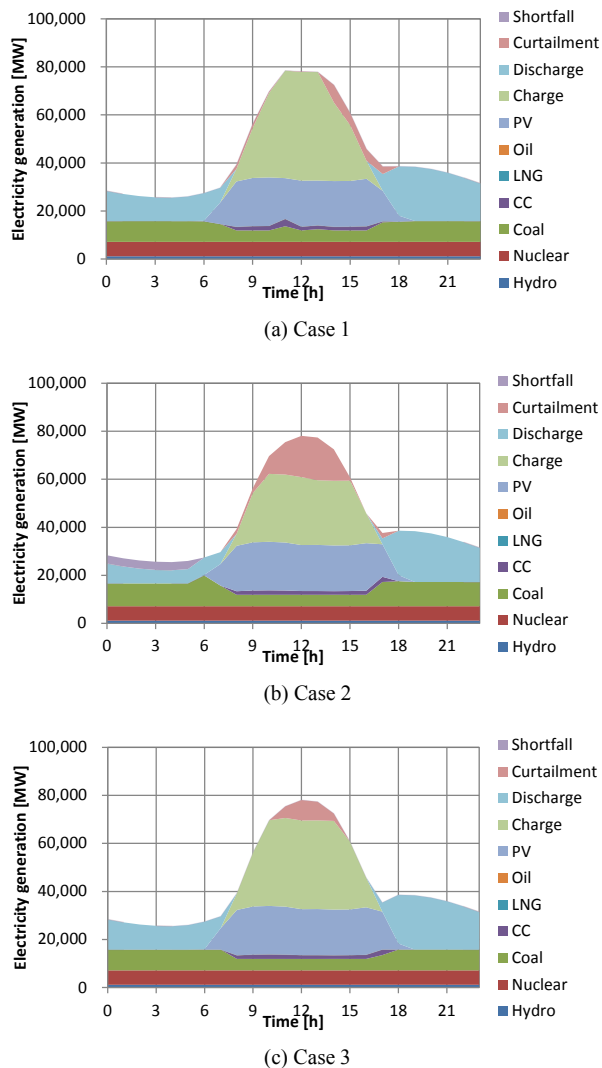


Figure 10. Daily load curve on March 22 (PV: 100 GW).

0 to 6 h because the UC during this period was determined under the assumption that the discharging power would be larger. Thus, the shortfall in Case 2 becomes larger than that in Case 1 when the installed capacity is extremely large, as shown in Fig. 2.

V. CONCLUSION

In this study, we proposed and evaluated a method for determining and updating BESS charging/discharging schedules and generator UCs. The one-year simulation results obtained using various installed PV capacities demonstrated the effectiveness with which the energy shortfall and PV curtailment can be reduced by updating the BESS schedule and UC based on more accurate forecasts. However, they also showed that both the shortfall and curtailment reductions are limited when the installed PV capacity is extremely large. In future work, we will improve the BESS scheduling method by extending the scheduling period from a day to several days and develop a method for the current day BESS operation to avoid not only power surplus, but also power shortfall.

REFERENCES

- [1] Ministry of Economy, Trade and Industry. Present status and promotion measures for the introduction of renewable energy in Japan. [Online]. Available: http://www.meti.go.jp/english/policy/energy_environment/renewable/
- [2] HARPS, System theory for harmonized power system control based on photovoltaic power prediction [Online]. Available: <http://harps-crest.jpn.org/en/index.php/>
- [3] Y. Hatanaka, Y. Suzuoki, T. Funabashi, T. Kato, M. Kurimoto, and Y. Manabe, "A study on evaluation of PVS forecast update accuracy from the viewpoint of unit commitment rescheduling," in *Int. Conf. on Electrical Engineering*, Okinawa, Japan, 2016.
- [4] Y. Ikeda, T. Ikegami, K. Kataoka, and K. Ogimoto, "A unit commitment model with demand response for the integration of renewable energies," in *2012 IEEE Power and Energy Society General Meeting*, San Diego, U.S., pp. 1-7, 2012.
- [5] California ISO. MRTU Market Elements Demand Response. [Online]. Available: <http://www.aiso.com/Documents/Presentation-MRTUMarketOverviewandTimeline.pdf>
- [6] T. Senjyu, T. Miyagi, S. A. Yousuf, N. Urasaki, and T. Funabashi, "A technique for unit commitment with energy storage system," *Int. J. Electr. Power Energ. Syst.*, 29(1), pp. 91-98, 2007.
- [7] M. K. C. Marwali, H. Ma, S. M. Shahidepour, and K. H. Abdul-Rahman, "Short term generation scheduling in photovoltaic-utility grid with battery storage," in *7th Int. Conf. on Power Industry Computer Applications*, Columbus, USA, 1997.
- [8] R. Moslemi, A. Hooshmand, and R. K. Sharma, "A machine learning based demand charge management solution," in *7th Innovative Smart Grid Technologies Europe*, Torino, Italy, 2017.
- [9] T. Masuta, D. Kobayashi., H. Ohtake, and N. H. Viet, "Evaluation of unit commitment based on intraday few-hours-ahead photovoltaic generation forecasts to reduce the supply-demand imbalance," in *8th Int. Renewable Energy Congress*, Amman, Jordan, 2017.
- [10] T. Masuta, J. G. da Silva Fonseca Jr., H. Ohtake, and A. Murata, "Application of battery energy storage system to power system operation for reduction in PV curtailment based on few-hours-ahead PV forecast," in *2016 Int. Conf. on Power System Technology*, Wollongong, Australia, 2016.
- [11] D. Kobayashi, T. Masuta, and H. Ohtake, "Coordinated operation scheduling method for BESS and thermal generators based on photovoltaic generation forecasts released every several hours," in *Proc. the 7th Innovative Smart Grid Technologies Asia*, Auckland, New Zealand, 2017.
- [12] T. Masuta and T. Fukumi, "Relationship between operating number of generators and supply-demand balance in power system with a large integration of renewable energy sources," in *Proc. Int. Conf. on Electrical Engineering 2016*, p. 90004.
- [13] T. Masuta, J. G. da Silva Fonseca, H. Ohtake, and A. Murata, "Study on Demand and Supply Operation Using Forecasting in Power Systems with Extremely Large Integrations of Photovoltaic Generation," in *Proc. the 4th Int. Conf. Sustain. Energy Technol.*, Hanoi, Vietnam, Nov. 14-17, 2016.
- [14] Tokyo Electric Power Company. TEPCO Electric Forecast [Online]. Available: <http://www.tepcoco.jp/en/forecast/html/index-e.html>
- [15] Japan Meteorological Business Support Center. [Online]. Available: <http://www.jmbc.or.jp/>
- [16] H. Ohtake, J. G. da Silva Fonseca Jr., T. Takashima., T. Oozeki, K. Shimose, and Y. Yamada, "Regional and seasonal characteristics of global horizontal irradiance forecasts obtained from the Japan Meteorological Agency mesoscale model," *Sol. Energy*, 116, pp. 83-99, 2015.
- [17] JMA Numerical Weather Prediction. [Online]. Available: <http://www.jma.go.jp/jma/jma-eng/jma-center/nwp/nwp-top.htm>